Trace Element Analysis using Resonant Laser Ablation

WATANABE, Kenichi
Department of Nuclear Engineering, School of Engineering, Nagoya University

IGUCHI, Tetsuo
Department of Nuclear Engineering, School of Engineering, Nagoya University

出版情報：Journal of Nuclear Science and Technology. 39 (4), pp.312-315, 2002-04. 日本原子力学会
バージョン：
権利関係：This is an Accepted Manuscript of an article published by Taylor & Francis inJournal of Nuclear Science and Technology on 07 Feb 2012, available online: "See DOI"

Trace Element Analysis using Resonant Laser Ablation

Kenichi WATANABE and Tetsuo IGUCHI

Department of Nuclear Engineering, School of Engineering, Nagoya University*

* Furo-cho, Chikusa-ku, Nagoya, 464-8603, Japan

Abstract

As a high efficiency solid sample analysis technique based on resonance ionization spectroscopy (RIS), Resonant Laser Ablation (RLA) is available. RLA combines Laser Ablation (LA) and RIS simultaneously with a single laser device. We have proposed the new dosimetry technique for a solid sample based on RLA.

We have attempted the detection of ^{26}Al ($T_{1/2}$: 7.2×10^5 y) produced in the high purity Al irradiated by 14 MeV neutrons at Fusion Neutronics Source (FNS), JAERI. Some interference effects are observed in the trace element detection experiments. These interference effects interrupt the detection of ^{26}Al. In conclusion, it is difficult that ^{26}Al is recognized clearly. We have mainly discussed the origins and elimination methods of these interference effects to detect the trace elements produced by nuclear reactions.

KEYWORDS: resonance ionization spectroscopy, resonance ionization mass spectrometry, laser ablation, resonant laser ablation, neutron dosimetry, ^{26}Al

和文抄録

高感度かつ元素（同位体）選択性をもつ共鳴イオン化分光法（Resonance ionization spectroscopy: RIS）に基づく高効率な固体試料分析法として、レーザーアブレーションと RIS を組み合わせ、これを 1 基のレーザー装置で同時に行う共鳴レーザーアブレーション法（Resonant Laser Ablation: RLA）が注目されている。本研究では、RLA を用いた新しい中性子ドシメトリー手法の開発を目的としている。

例として、日本原子力研究所（JAERI）の核融合炉物理用中性子源施設(FNS)にて、高純度 Al に 14 MeV 中性子の重照射（1.0×10^{17} n/cm^2）を行い、生成した ^{26}Al（$T_{1/2}$: 7.2×10^5 y）を RLA により検出することを試みた。RLA を用いた微量元素検出では、^{26}Al 検出を妨げる様々な干渉効果が観測された。今回は、これらの効果の原因及びその解決策について検討を行った。

I. Introduction

Resonance Ionization Mass Spectroscopy (RIMS), which combines Resonance Ionization Spectroscopy (RIS) with mass spectrometry, is high sensitive mass spectrometry without isobaric interference, because the ionization with the elemental (isotopic) selectivity and high efficiency is practicable with resonance ionization scheme. Recently RIMS has developed and has been used to demonstrate single atom detection. Therefore, RIMS is available for low-level isotope analysis such as age dating. [1] [2]

One of the new applications of RIMS is the neutron dosimetry technique as an alternative of conventional activation analysis. The new neutron dosimetry technique based on RIMS is based on direct detection of trace nuclides produced by neutron irradiation. The dosimetry technique based on RIMS is available for long-lived radionuclides and/or stable nuclides. Other direct detection techniques, such as ICP-MS and AMS, are also promising candidates, but they have difficulty on isobaric interference, which can be easily avoided in RIMS.

To improve the sensitivity of RIMS, it needs to squeeze many atoms into effective ionization volume. On the other hand, RIMS is the analysis method for a gaseous sample and needs a vaporization procedure to analyze a solid sample. We have adopted laser ablation (LA) method for vaporization of a solid sample. As a high sensitive analysis technique for a solid sample, we have adopted resonant laser ablation (RLA), which combines LA and RIS simultaneously with a single laser device.[3][4] In RLA, the effective ionization volume is very close to the spot of LA and the evaporated atoms are confined into the ionization volume. We have proposed the new dosimetry technique for a solid sample based on RLA.

As an illustration of the detection of trace long-lived radionuclides, we are attempting the detection of ^{26}Al ($T_{1/2}$: 7.2×10^5 y) produced by $^{27}Al(n,2n)$ reaction

in high energy neutron fields. Al material is promising low-activation material for fusion reactors or accelerators. The determination of trace long-lived radionuclides produced in Al material in fusion reactors is quite important from the viewpoint of reduction of the radioactive waste. It is difficult for the activation analysis to detect ^{26}Al due to its long half-life. The direct detection techniques without the elemental selectivity are affected by the isobaric interference of ^{26}Mg, which tends to be contained in the Al material as an impurity.

It turned out that RLA technique has the capability for the detection of ^{26}Al through the estimation of the detection limit and elemental selectivity.(5) We practically have attempted the detection of ^{26}Al produced in the high purity aluminum irradiated by 14 MeV neutrons at Fusion Neutronics Source(FNS), JAERI. Some interference effects are observed in these experiments. We have mainly discussed the origins and elimination methods of these interference effects to detect trace elements produced by nuclear reactions.

II. Experimental Setup

Figure 1 shows the schematic of the present experimental system, which consists of one tunable dye laser pumped by a pulsed Nd: YAG laser and reflectron TOF mass spectrometer with a field-free drift region approximately 150 cm long and a microchannel plate (MCP) ion detector. The dye laser output was split into two beams for LA and RIS, respectively. The Nd: YAG laser, which is normally used for pumping the dye laser, can also be used for LA. The RIS effective ionization volume was as close as possible to the LA spot. The RIS laser was delayed to the LA laser for 50 ns, because it needs a finite time for diffusion of the vapor evaporated by LA. The bandwidth of the dye laser is 0.14 cm^{-1}, the laser pulse duration 10 ns and the repetition rate 10 Hz, respectively. The laser beams

were focused at the ionization area with the diameter of 100 μm. The typical laser output energy was 500 μJ/pulse (≈6×10^{8} W/cm^2) for RIS and 50 μJ/pulse (≈6×10^{7} W/cm^2) for LA.

As a sample, high purity aluminum (99.999 %) rod was used. This sample was irradiated by 14 MeV neutrons with the fluence of 1.0×10^{17} n/cm^2 at FNS, JAERI. It is estimated that ^{26}Al in this sample is produced with the concentration of 0.6 ppb.

Fig. 1

III. Results and Discussion

The detection limit of RLA for Al was estimated to be 1 ppm per one laser shot with the gain of 10^3 for Al to Mg, that is, Al ion yield is 10^3 times larger than Mg ion yield.(5) The ^{26}Al content in a sample with 0.1 ppb can be detected by accumulating 10^4 laser shots (i.e. 17 min). The concentration of ^{26}Al in the Al sample irradiated by 14 MeV neutrons (1.0×10^{17} n/cm^2) is 0.6 ppb and the concentration of ^{26}Mg contained in the Al sample as an impurity is less than 1 ppm. It is found that RLA technique has the capability for the detection of ^{26}Al through the estimation of the detection limit and elemental selectivity.

Figure 2 shows the schematic of the electrodes of the TOF mass spectrometer. Figure 3 gives the TOF mass spectra for 40000 laser shots from Al sample irradiated by 14 MeV neutrons when the voltages shown in Table 1 are applied to the TOF electrodes. On only resonance wavelength for Al, there are the peaks with m/z = 20.6, 19.2 etc. and the tailed shape on the low m/z value side of the peak of ^{27}Al. The peak of ^{26}Al is submerged in these peaks and the tailed shape near the ^{27}Al peak and eventually cannot be recognized clearly. To discuss the origins of these peaks, we investigated the response of these peaks for the RIS laser. Figure 4 shows the dependence of the ion yield of these peaks on the RIS

laser wavelength. From Fig. 4, the ions forming these peaks are considered to be generated by resonance ionization process as well as ^{27}Al or some process caused by ^{27}Al ions.

Table 1
Fig. 2. 3. 4

We assume that the ions forming the peaks in the Fig. 3 are secondary ^{23}Na, ^{27}Al ions etc., which is sputtered by ^{27}Al ions from the reflectron electrode VR1 and accelerated by the reflectron and eventually detected. These Al and Na are considered to be deposited by the ion beams generated by RIS, because the electrodes are stainless steel. Figure 5 gives the dependence of the flight time of these ions on the applied voltage to VR1. As a result, the flight time of these ions agrees with the expected one. We conclude that our assumption is correct.

Fig. 5

The tailed shape is considered to be caused by fragments of cluster ions that fragment in the acceleration region of the TOF mass spectrometer. It is considered that the clusters are produced by LA and ionized by the collision with ^{27}Al ions. The mass spectra simulated by Monte Carlo method are shown in Fig. 6 when $^{27}Al_2^+$ and $^{27}Al_2^{3+}$ ions are assumed to fragment in the TOF mass spectrometer. The fight time of $^{27}Al^+$ ions that are the fragments of $^{27}Al_2^+$ ions that fragment in the acceleration region is longer than that of $^{27}Al^+$ ions produced in the form of $^{27}Al^+$ from the start (that is normal $^{27}Al^+$ ions), because the ratio of mass to electric charge of $^{27}Al_2^+$ is larger than that of $^{27}Al^+$ and the acceleration is small before the fragmentation. In contrast, the fight time of $^{27}Al^+$ ions that are the fragments of $^{27}Al_2^{3+}$ is shorter than that of normal $^{27}Al^+$ ions. $^{27}Al_2^+$ and $^{27}Al_2^{3+}$ are typical instance of $^{27}Al_m^{n+}(m>n)$ and $^{27}Al_m^{n+}(m<n)$, respectively. For $^{27}Al_m^{n+}(m=n)$ ions, the flight time is equal to $^{27}Al^+$ due to the same ratio of mass to electric charge. In this calculation, for instance, we assumed that the lifetime of cluster ions is 1 μsec, because metal clusters sputtered by ion beam have the lifetime of the order of μsec[6]. The tailed shapes on the high and low m/z value

side of the peak of ^{27}Al are formed by fragments of $^{27}Al_m^{n+}$(m>n) and $^{27}Al_m^{n+}$(m<n) ions that fragment in the acceleration region, respectively. **Fig. 6**

Figure 7 gives the mass spectra for 30000 laser shots under the condition that the ions is not sputtered from the electrode VR1, which is achieved by applying the voltages shown in Table 2 to the TOF electrodes. In Fig. 7, the confusing peaks vanished, but the peak of ^{26}Al is still submerged in the tailed shape near the ^{27}Al peak. In conclusion, it is difficult that ^{26}Al is recognized clearly. If this interference effect can be eliminated, it is expected that the ^{26}Al can be detected clearly. For example, the interference effect for the cluster ions can be eliminated by use of quadrupole mass spectrometer (QMS) instead of TOF mass spectrometer, because QMS is not affected by the fragments of cluster ions that fragment in the mass spectrometer. **Fig. 7** **Table 2**

In addition, it is also considered that the detection of ^{26}Al is interrupted by the space charge effect. The space charge effect is the effect that densely produced ions are diffused by the Coulomb repulsive of themselves. The space charge effect decreases the detection efficiency. One of the solvents of this problem is the suppression of the production of ^{27}Al ions using the isotope shift of the transition wavelength. Unfortunately, our laser system cannot distinguish the isotope shift between ^{26}Al and ^{27}Al because the bandwidth of our laser is broader than the isotope shift.

IV. Conclusion

We have proposed the new dosimetry technique for a solid sample based on RLA. For instance, we have attempted the detection of ^{26}Al produced in the high purity aluminum irradiated by 14 MeV neutrons at FNS, JAERI.

It is found that there are some interference effects in the trace element

detection experiments, which are caused by the secondary ions sputtered by ^{27}Al from the reflectron electrode and by fragments of the cluster ions that fragment in the acceleration region of the TOF mass spectrometer. The secondary ions sputtered from the reflectron can be eliminated by changing the applied voltage to the reflectron. However, the peak of ^{26}Al is still submerged by the interference effect of the cluster ions. In conclusion, it is difficult that ^{26}Al is recognized clearly. If this interference effect can be eliminated, it is expected that the ^{26}Al can be detected clearly.

As the future works, we will try to replace TOF-MS with QMS to eliminate the cluster ion effect. To eliminate the space charge effect, it is effective that the production of ^{27}Al ions is suppressed by the isotope shift of the transition wavelength using a more narrow bandwidth laser system such as a laser diode.

Acknowledgements

We gratefully acknowledge T. Nishitani of FNS, JAERI for irradiating the Al sample by 14 MeV neutrons.

References

(1) G. S. Hurst, M. G. Payne, S. D. Kramer, et al., “Counting The Atoms,” *Phys. Today*, **33**, 24-29 (1980).

(2) G. S. Hurst, M. G. Payne, S. D. Kramer, et al., “Method for Counting Noble Gas Atoms with Isotopic Selectivity,” *Rep. Prog. Phys.*, **48**, 1333-1370 (1985).

(3) C. G. Gill, A. W. Garrett, P. H. Hemberger, et al., “Selective Laser

Ablation/Ionization for Ion Trap Mass Spectrometry: Resonant Laser Ablation," *Spectrochimi. Acta B*, **51**, 851-862 (1996).

(4) J. E. Anderson, T. M. Allen, A. W. Garrett, et al., "Resonant Laser Ablation: Mechanisms and Applications," *AIP Conf. Proc.*, **388**, 195-198 (1997).

(5) K. Watanabe, T. Iguchi, "Optimization of Trace Element Analysis using Resonant Laser Ablation," *AIP Conf. Proc.*, **584**, 135-140 (2001)

(6) N. Kh. Dzhemilev, U. Kh. Rasulev, S. V. Verkhoturov, "The Fragmentation of Sputtered Cluster Ions and Their Contribution to Secondary Ion Mass-Spectra," *Nucl. Instrum. Methods B*, **29**, 531-536 (1987)

Table 1 Applied Voltage to the electrodes of the TOF mass spectometer.

Electrode	VA1	Vs	VA2	VR1	VR2
Voltage [V]	4000	3500	3000	3000	4000

Table 2 Applied Voltage to the electrodes of the TOF mass spectometer. In this case, the ions is not sputtered from the electrode VR1.

Electrode	VA1	Vs	VA2	VR1	VR2
Voltage [V]	3130	2500	2000	3300	3400

FIGURE CAPTIONS

Fig. 1 Schematic of the experimental apparatus.

Fig. 2 Schematic of the electrodes of the TOF mass spectrometer.

Fig. 3 TOF mass spectra for 40000 laser shots from Al sample irradiated by 14 MeV neutrons.

Fig. 4 RIS laser wavelength dependence of the ion yield corresponding to the peaks with m/z = 19.2, 20.6 (Peak A, B, respectively) in Fig. 3.

Fig. 5 Dependence of the flight time of the ions sputtered from the reflectron electrode VR1 on the applied voltage to VR1. Dots and lines are the experimental and calculated results, respectively. Thin line and thin broken line are the flight time of ^{27}Al and ^{23}Na, respectively. Thick line and thick broken line are the sum of the flight time of ^{27}Al ions from the sample position to the VR1 electrode and the flight time of secondary ^{27}Al and ^{23}Na ions from VR1 to the ion detector, respectively.

Fig. 6 Mass spectra simulated by Monte Carlo method when $^{27}Al_2^+$ and $^{27}Al_2^{3+}$ ions are assumed to fragment in the TOF mass spectrometer. The applied voltage to the electrodes of the TOF mass spectrometer is shown in Tables 2 and the lifetime of the cluster ions is assumed to be 1 μsec.

Fig. 7 TOF mass spectra for 30000 laser shots under the condition that the ions are not sputtered from the electrode VR1.

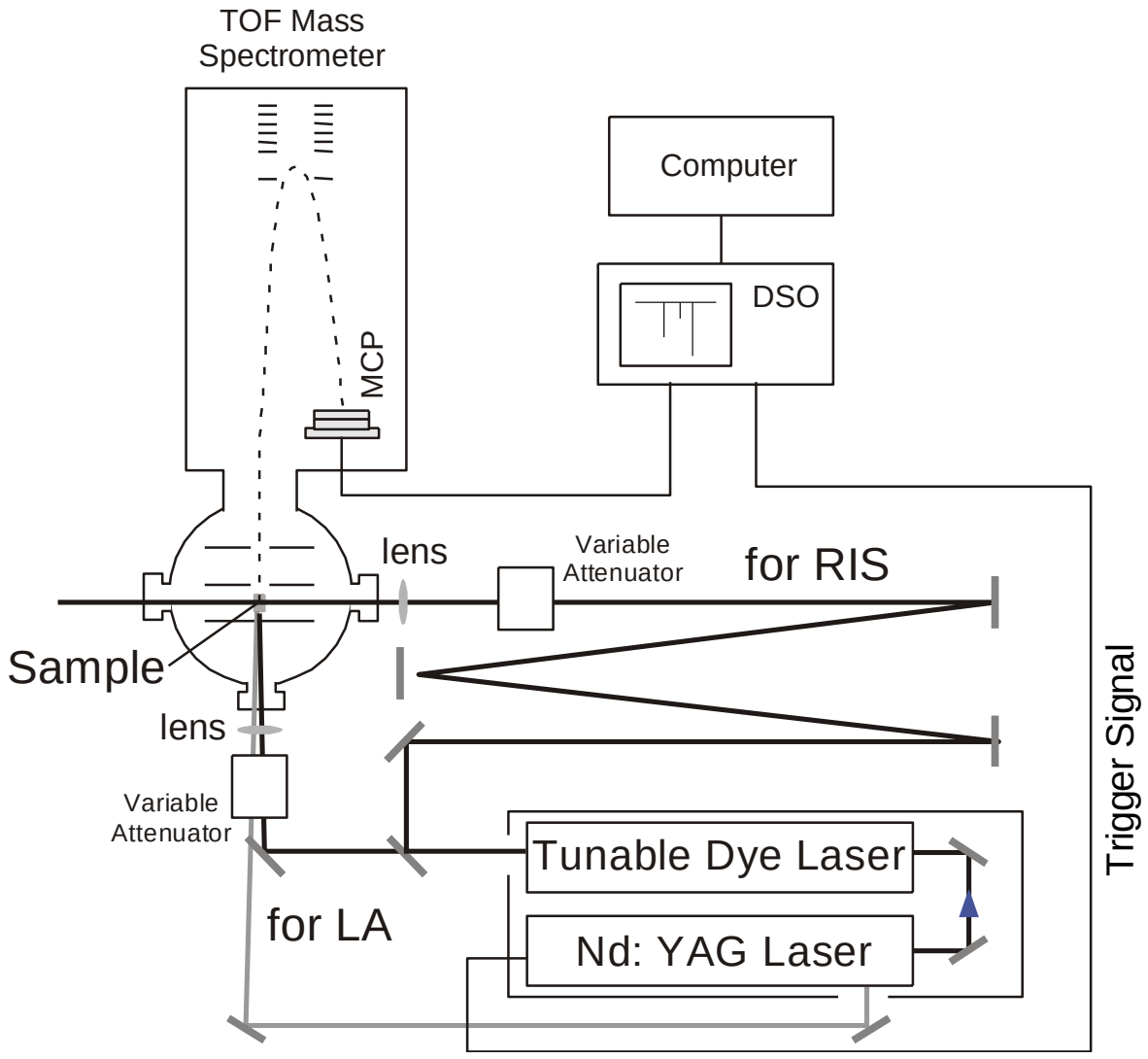

Fig. 1 K. Watanabe et al.
" Development of Failed Fuel Detection and Location Technique using Resonance Ionization Mass Spectrometry "

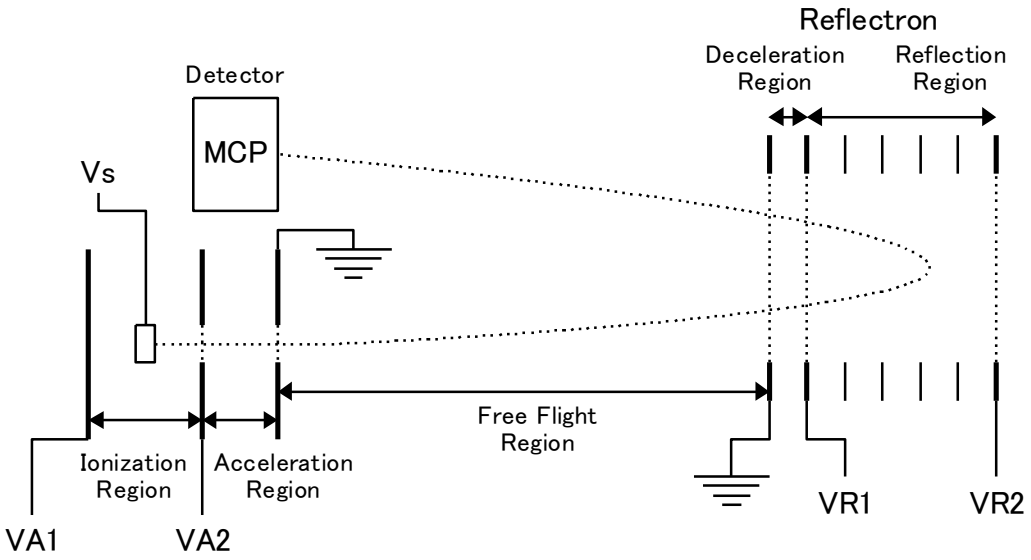

Fig. 2 K. Watanabe et al.

" Development of Failed Fuel Detection and Location Technique using Resonance Ionization Mass Spectrometry "

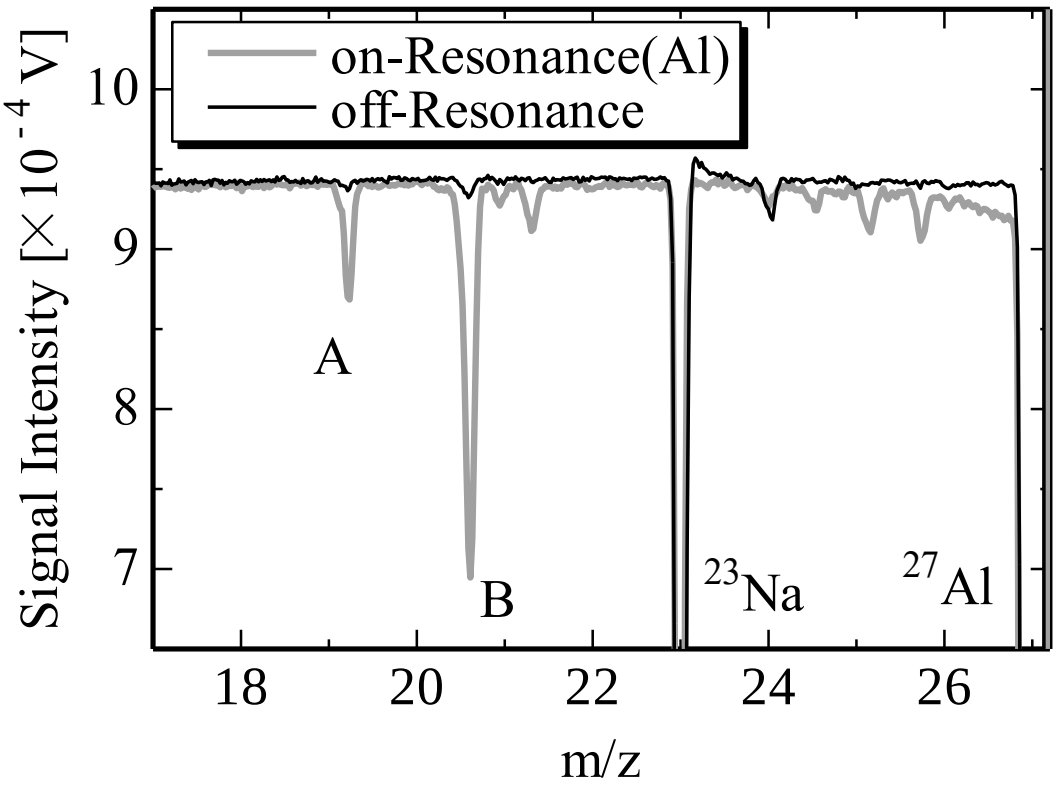

Fig. 3 K. Watanabe et al.

" Development of Failed Fuel Detection and Location Technique using Resonance Ionization Mass Spectrometry "

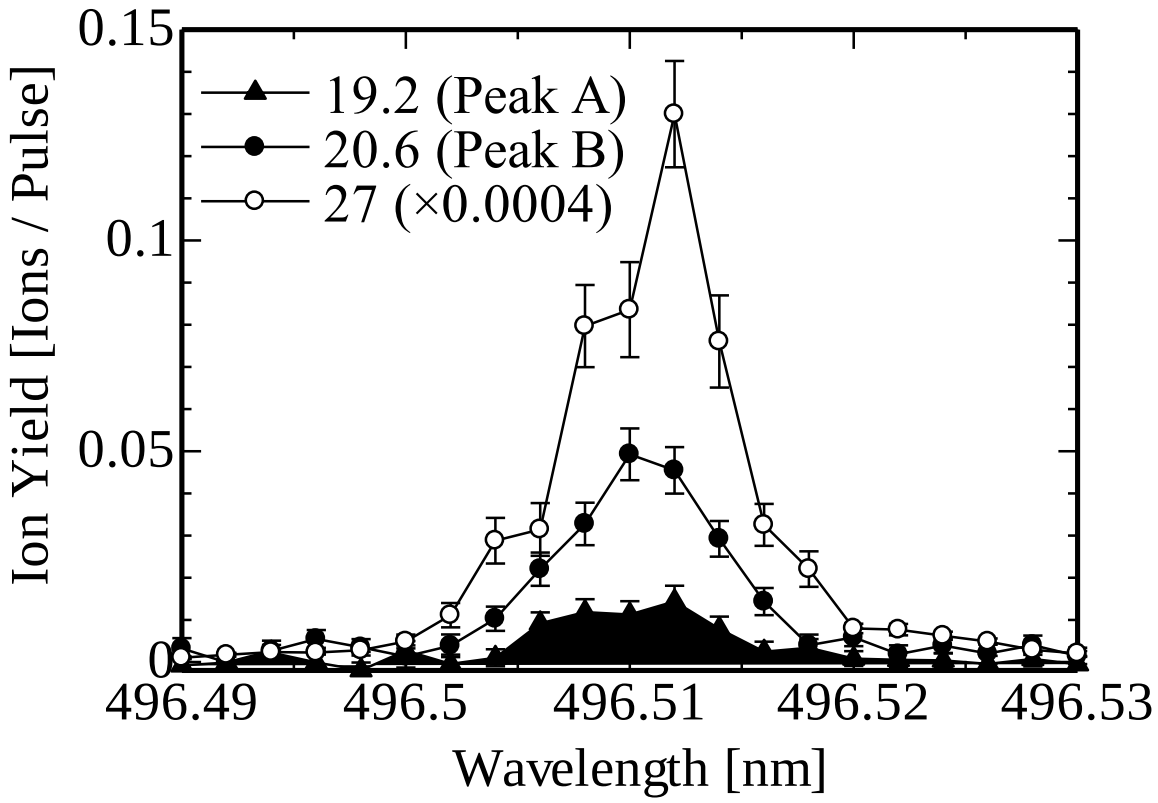

Fig. 4 K. Watanabe et al.

" Development of Failed Fuel Detection and Location Technique using Resonance Ionization Mass Spectrometry "

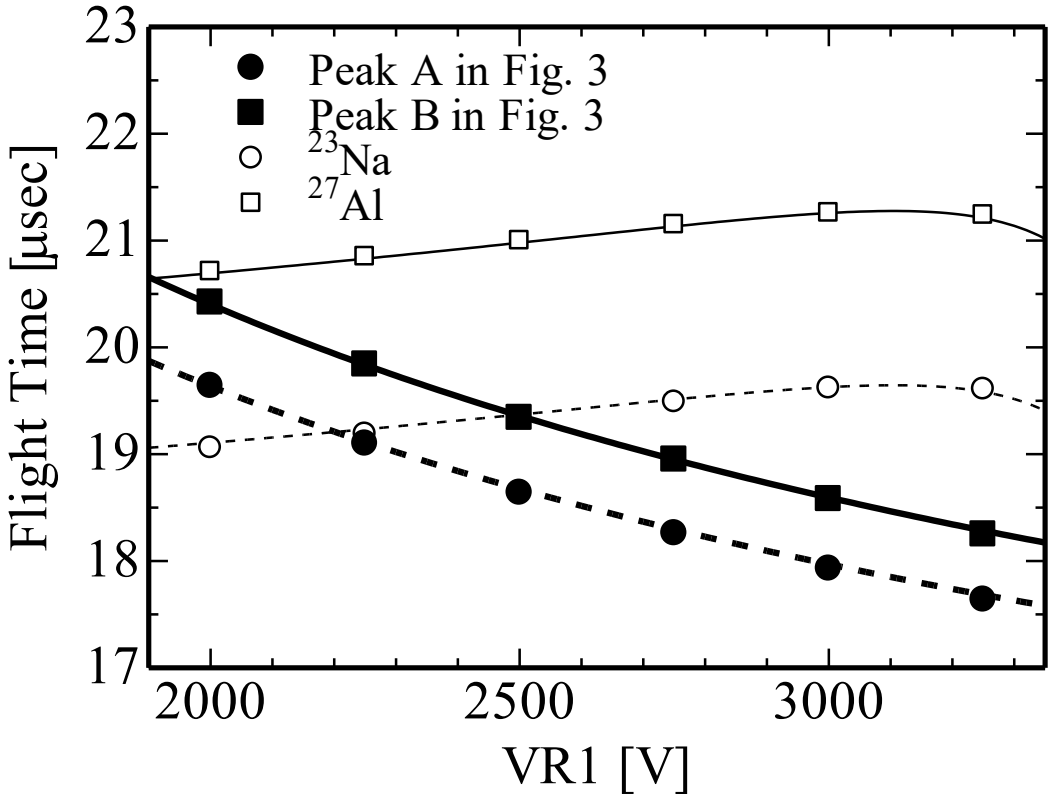

Fig. 5 K. Watanabe et al.

" Development of Failed Fuel Detection and Location Technique using Resonance Ionization Mass Spectrometry "

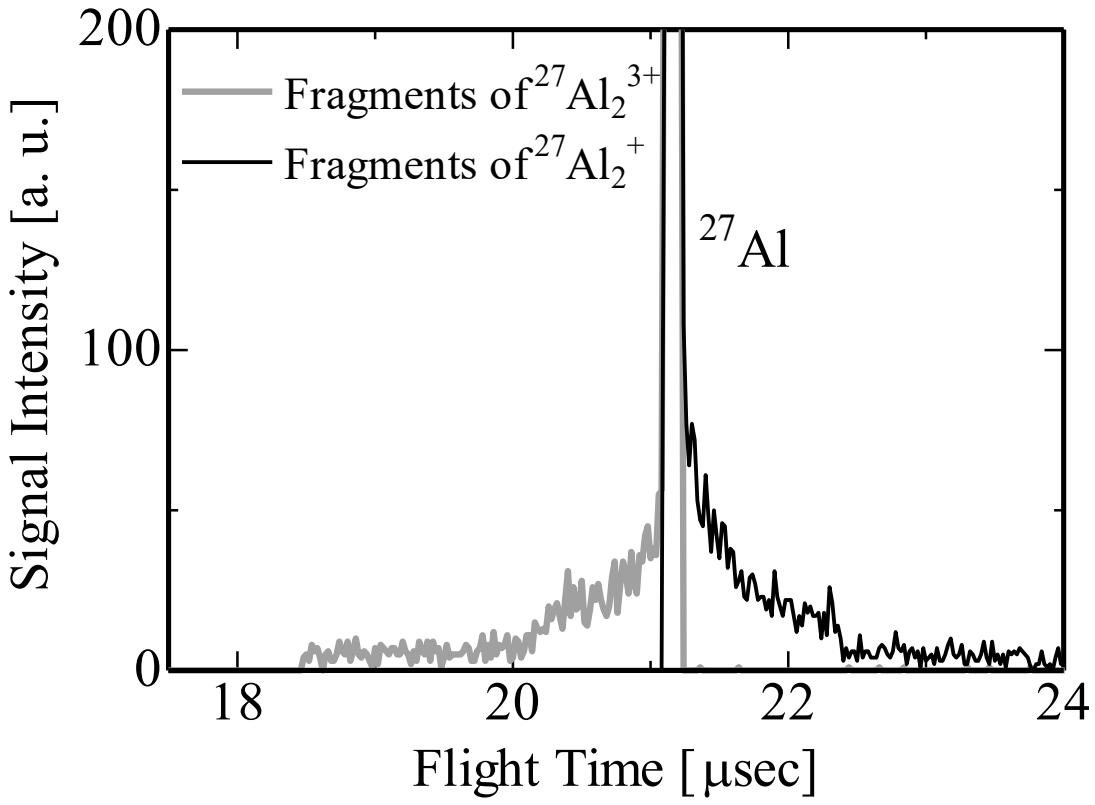

Fig. 6 K. Watanabe et al.

" Development of Failed Fuel Detection and Location Technique using Resonance Ionization Mass Spectrometry "

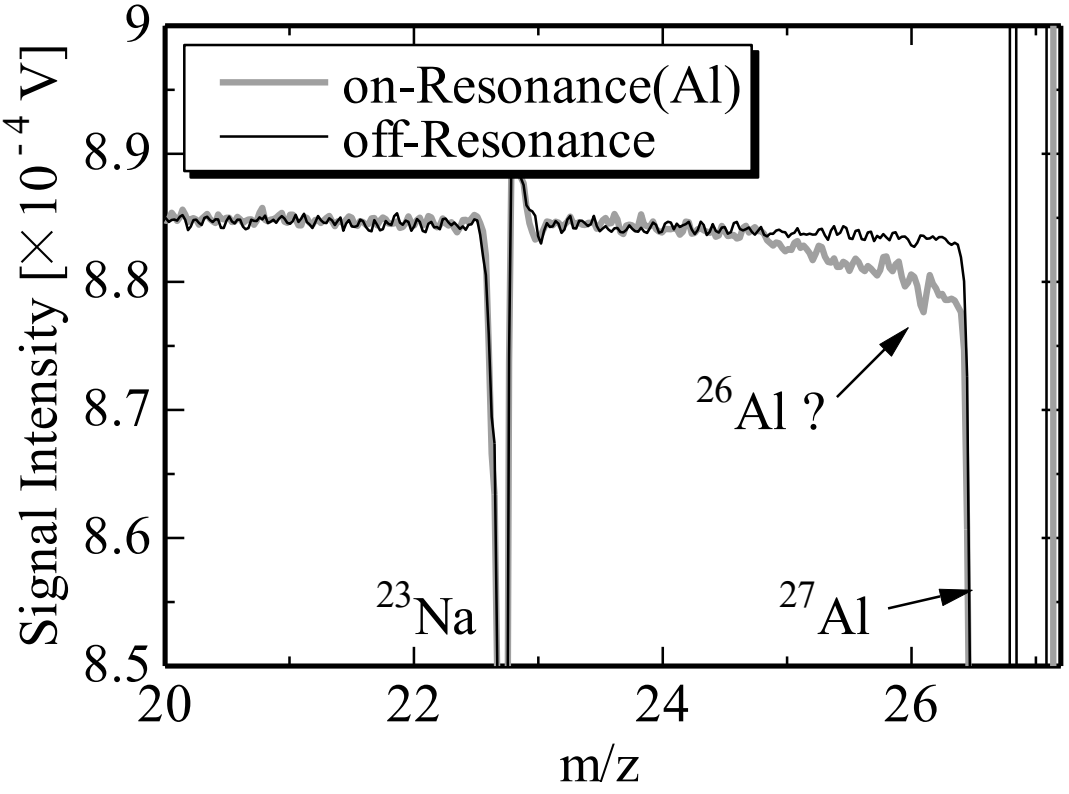

Fig. 7 K. Watanabe et al.

" Development of Failed Fuel Detection and Location Technique using Resonance Ionization Mass Spectrometry "